Molecular Crystals and Liquid Crystals

Publication details, including instructions for authors and subscription information:
http://www.tandfonline.com/loi/gmcl20

Structural Peculiarities of Triblock Copolymers Containing Poly(Ethylene Oxide) and Polyacrylamide

S. V. Fedorchuk [a], T. B. Zheltonozhskaya [a], N. M. Permyakova [a], Y. P. Gomza [b], S. D. Nessin [b] & V. V. Klepko [b]

[a] Taras Shevchenko Kyiv National University, Faculty of Chemistry, Department of Macromolecular Chemistry, Kyiv, Ukraine

[b] Institute for Macromolecular Chemistry of National Academy of Sciences of Ukraine, Kyiv, Ukraine

Version of record first published: 10 Jun 2010

To cite this article: S. V. Fedorchuk, T. B. Zheltonozhskaya, N. M. Permyakova, Y. P. Gomza, S. D. Nessin & V. V. Klepko (2008): Structural Peculiarities of Triblock Copolymers Containing Poly(Ethylene Oxide) and Polyacrylamide, Molecular Crystals and Liquid Crystals, 497:1, 268/[600]-281/[613]

To link to this article: http://dx.doi.org/10.1080/15421400802463092

Mol. Cryst. Liq. Cryst., Vol. 497, pp. 268/[600]–281/[613], 2008

ISSN: 1542-1406 print/1563-5287 online
DOI: 10.1080/15421400802463092

Taylor & Francis
Taylor & Francis Group

Structural Peculiarities of Triblock Copolymers Containing Poly(Ethylene Oxide) and Polyacrylamide

S. V. Fedorchuk[1], T. B. Zheltonozhskaya[1], N. M. Permyakova[1], Y. P. Gomza[2], S. D. Nessin[2], and V. V. Klepko[2]

[1]Taras Shevchenko Kyiv National University, Faculty of Chemistry, Department of Macromolecular Chemistry, Kyiv, Ukraine
[2]Institute for Macromolecular Chemistry of National Academy of Sciences of Ukraine, Kyiv, Ukraine

The morphology of the triblock copolymers (TBC) containing chemically complementary poly(ethylene oxide) ($M_{vPEO} = 3 \cdot 10^3 \div 1 \cdot 10^5$) and polyacrylamide ($M_{PAAm} = 4.5 \cdot 10^4 \div 9.07 \cdot 10^5$) of different chain lengths is studied. The loss of the PEO ability to crystallize in TBC at $M_{vPEO} \leq 4 \cdot 10^4$ is established. At the same time, PEO blocks with $M_v = 1 \cdot 10^5$ form small crystalline domains in the TBC structure, but their crystallinity degree turns out to be by 2.8 times less than that in individual poly(ethylene oxide). A microphase separation in amorphous regions of the TBC structure at high values of M_{PAAm} is revealed. It is shown that the main reason for the effects observed is the formation of a complex between PEO and PAAm blocks by hydrogen bonds.

Keywords: intramolecular polycomplex; poly(ethylene oxide); polyacrylamide; structure; triblock copolymer

INTRODUCTION

Modification of physicochemical properties and structures of homopolymers by covalent coupling of them with different polymer components is well-known. Majority of studies in this field is devoted to the block copolymers with thermodynamically immiscible or limitedly miscible polymer components. These compounds can form "supercrystalline" structures in a bulk state [1] and various micellar and

Address correspondence to S. V. Fedorchuk, Taras Shevchenko Kyiv National University, Faculty of Chemistry, Department of Macromolecular Chemistry, 64, Vladimirskaya str., Kyiv 01033, Ukraine. E-mail: sergey_fedorchuk@ukr.net

vesicular structures in a solution [2,3]. However, the block copolymers with chemically complementary components, capable to form the system of cooperative non-covalent bonds, namely, electrostatic in ampholytic (or zwitter-ionic) block copolymers [4] or hydrogen bonds in the block and graft copolymers based on nonionic polymers and polyacids [5,6], are of significant interest. These block copolymers belong to the class of intramolecular polycomplexes (IntraPC) and have many potential applications as multifunctional membranes, binders in biotechnologies and medicine, and also as efficient flocculants and the agents of a drag reduction of a turbulent flow [7]. At the same time, their structure in a bulk state and in a solution is not enough studied.

It was shown earlier [8] that polyacrylamide (PAAm) and poly(ethylene oxide) (PEO) are a pair of chemically complementary polymers which form the hydrogen-bound intermolecular polycomplex (InterPC) at their mixing in an aqueous medium. Using these data, we begin a systematic study of a bulk structure and the hydrogen bond system in the PAAm-*b*-PEO-*b*-PAAm triblock copolymers (TBC) with variable length of the central and side blocks [9], as well as consider the formation of IntraPC in the copolymer macromolecules. In order to obtain the detailed information about the effect of the PEO and PAAm block length on the copolymer bulk structure, a number of TBCs investigated was expanded in the present work. Moreover, in addition to differential scanning calorimetry (DSC), two additional structurally sensitive methods such as wide-angle and small-angle X-ray scattering (WAXS and SAXS) are also used for this purpose.

EXPERIMENTAL

The triblock copolymers were synthesized by free-radical block copolymerization of acrylamide (AAm) from "Merck" (Germany) with poly(ethylene glycols) of different molecular weights: $M_{v\mathrm{PEG}} = 3 \cdot 10^3$ (PEG1), $6 \cdot 10^3$ (PEG2), $1.5 \cdot 10^4$ (PEG3), $4 \cdot 10^4$ (PEG4) and $1 \cdot 10^5$ (PEG5) which were received from the same firm. Terminal hydroxyl groups of PEG were activated by Ce^{IV} ions according to the following scheme:

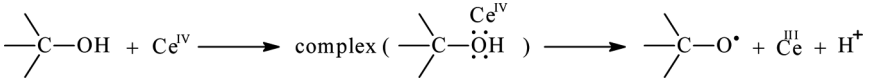

Block copolymerization was performed for 24 h in an inert atmosphere at 25°C, using the following constant molar ratios of reagents: $[Ce^{IV}]/[PEG] = 2$ and $[Ce^{IV}]/[AAm] = 1 \cdot 10^{-3}$. Gel-like products were

diluted by deionized water, reprecipitated by acetone, and freeze dried. Two series of TBC samples: TBC1–5 and TBC6–7 were obtained. In the second series, the total concentration of all the reagents was enhanced by a factor of 1.53. Homopolymerization of AAm was carried out under the same experimental conditions, using ethanol instead PEG ($[Ce^{IV}]/[C_2H_5OH] = 1$) [10]. According to the viscosimetry data, the molecular weight of a PAAm sample synthesized was equal to $M_v = 6.31 \cdot 10^5$. Molecular parameters of TBCs found by elemental analysis are submitted in Table 1.

It is seen that, in both the copolymer series, the increase in the PEO length is accompanied by a growth of the PAAm block length. At the same time, the length of a PAAm block appreciably grows with increase in the total concentration of the reagents in synthesis.

A microcalorimeter DSC-210 and a thermoanalizer "Du Pont" were used in DSC studies. In order to define the thermodynamic parameters of structural transitions, the instrument was calibrated by indium and zinc. The sapphire crystal was heated simultaneously with each polymer sample (Fig. 1) in order to recalculate the heat flow curves in the dependences of the specific heat capacity (C_p) versus the temperature by the following relation:

$$C_p(T) = C_p^0 \cdot \frac{l}{l^0} \cdot \frac{m^0}{m}.$$

Here, C_p^0 is the specific heat capacity of sapphire at a given temperature; l^0 and l are the distances between thermograms of sapphire (and polymer) and the base line at the same temperature; m^0 and m

TABLE 1 The Main Molecular Parameters of PAAm-*b*-PEO-*b*-PAAm Triblock Copolymers

Copolymer	$M_{v\mathrm{PEO}} \cdot 10^{-5}$	$M_{\mathrm{PAA}} \cdot 10^{-5}$	$M_{\mathrm{TBC}} \cdot 10^{-5}$	$w_{\mathrm{PEO}}{}^a$,%	n^b
TBC1	0.03	0.45	0.94	3.2	9.4
TBC2	0.06	0.54	1.14	5.2	5.6
TBC3	0.15	1.21	2.57	5.8	5.0
TBC4	0.40	3.18	6.76	5.9	4.9
TBC5	1.00	9.07	19.14	5.2	5.6
TBC6	0.15	2.30	4.75	3.2	9.5
TBC7	0.40	8.33	17.06	2.3	12.9

[a]The weight part of PEO in the copolymers.

[b]The ratio between units of PAA and PEO blocks in the copolymers, base-mole$_{\mathrm{PAA}}$/base-mole$_{\mathrm{PEO}}$.

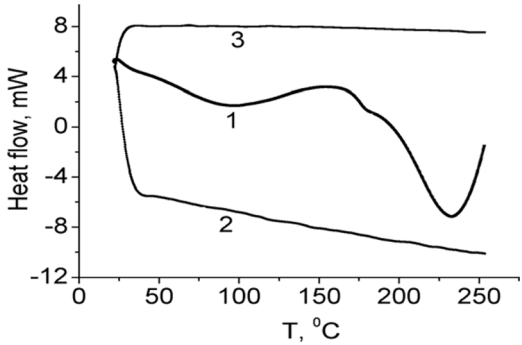

FIGURE 1 Example of DSC thermograms for TBC1 (2-nd scan) – 1 and the sapphire crystal – 2. Base line – 3.

are the weights of sapphire (61.66 mg) and polymer, respectively. Polymer samples (4–6 mg) were dried in a vacuum case at 80°C and a vacuum-desiccator above $CaCl_2$. Further, the samples were placed in open capsules, cooled by liquid nitrogen, and heated with a rate of 16 degree/min.

Structural studies of the polymers by WAXS were carried out, by using an X-ray diffractometer DRON-2.0 [11]. Polymer films with $l = 80 \div 115$ μm were cast from aqueous solutions on the Teflon surface and dried in a vacuum case for one week. The film piles with thickness ~1 mm were used for measurements. The monochromatic Cu-K_α radiation with $\lambda = 0.154$ nm filtered by Ni was provided by an IRIS-M7 generator at an operating voltage of 30 kV and a current of 30 mA. The scattering intensities were measured by a scintillation detector scanning in 0.2°-steps over the range of angles of 3–40°. Diffraction curves obtained were reduced to equal intensities of the primary beam and equal values of the scattering volume by the usual technique [11].

SAXS experiments with TBCs and PAAm were conducted on an automated Kratky slit-collimated camera. Here, the copper anode emission monochromated by total internal reflection and a nickel filter was used. The intensity curves were recorded in the step-scanning mode of a scintillation detector in the interval of scattering angles $2\theta = 0.03$–$4.0°$, which corresponds to the values of the wave vector, $q = 4\pi \sin\theta/\lambda$, from 0.022 to 2.86 nm^{-1}. Thus, studying the microheterogeneous domains with a characteristic dimension (evaluated as $2\pi/q$) from 2 to 280 nm was possible. The preliminary processing of SAXS profiles was carried out by using the FFSAXS-3 program [12]. To reduce the SAXS data to the absolute scale, a standard Lapolene

sample was used. In order to calculate the microphase structure parameters, the raw intensity curves were smoothed, corrected for parasitic scattering, and desmeared.

RESULTS AND DISCUSSION

DSC thermograms (the 1-st and 2-nd scans) are shown in Figure 2. Thermograms of the amorphous PAAm and all the TBCs (Fig. 2a, f–j) contained an intense endothermic peak of water evaporation. This peak didn't completely disappear in the 2-nd scan (after the additional "preliminary drying"). Such a behavior was caused by a high hydrophility of PAAm chains which "collect" water even at the polymer sample transferring from a desiccator to the instrument.

The thermogram of PAAm (Fig. 2a) contained also one heat capacity jump corresponding to the glass transition. Parameters of the transition such as T_g, ΔT_g, and ΔC_p are shown in Table 2. DSC thermograms of PEG didn't demonstrate a glass transition. They contained only intense peaks of the crystal phase melting (Fig. 2b–e). Characteristics of the melting process (T_m, ΔT_m, and ΔT_m) and the crystallinity degree (X_c) calculated for PEG with different M_v are submitted in Table 2.

The T_m, ΔH_m, and X_c values decreased in the 2-nd scan by 3–5°C, 2–16.5 J/g, and 4–9%, respectively. This effect was conditioned by a sharp cooling (~300 degree/min) of the samples from a melt (after the 1-st scan), which prevents the formation of a highly ordered crystal structure.

DSC data for TBCs (Fig. 2f–j, Table 2) were considered in two aspects: i) changing in the crystalline state of PEO in TBCs, depending on the molecular weight of blocks, and ii) changing in the amorphous phases. It was shown that PEO blocks with $M_v \leq 4 \cdot 10^4$ in TBC1–4 completely lost their ability to crystallize. Unlike this, PEO blocks with $M_v = 1 \cdot 10^5$ in TBC5 formed small crystalline domains, but their X_c sharply decreased as compared to that of the initial PEG sample (PEG4), namely, by 2.8 times according to the data for the 1-st scan and by 7.9 times by the data for the 2-nd scan. Additionally, T_m values decreased by 10°C for these micro- or nanocrystalline domains.

There are two possible reasons for the effects observed: i) a placement of the crystallizable block in TBC between two long amorphous blocks [6,13–15]; ii) complexation between the blocks [16,17]. On the one hand, the fact that even long PEO blocks ($M_{\mathrm{PEO}} \sim 5 \cdot 10^4$) lose their ability to crystallize in the triblock copolymers PMMA-*b*-PEO-*b*-PMMA (with no interacting components), when the length of PMMA blocks exceeded some critical value ($M^*_{\mathrm{PMMA}} \sim 5 \cdot 10^3$), is well-known

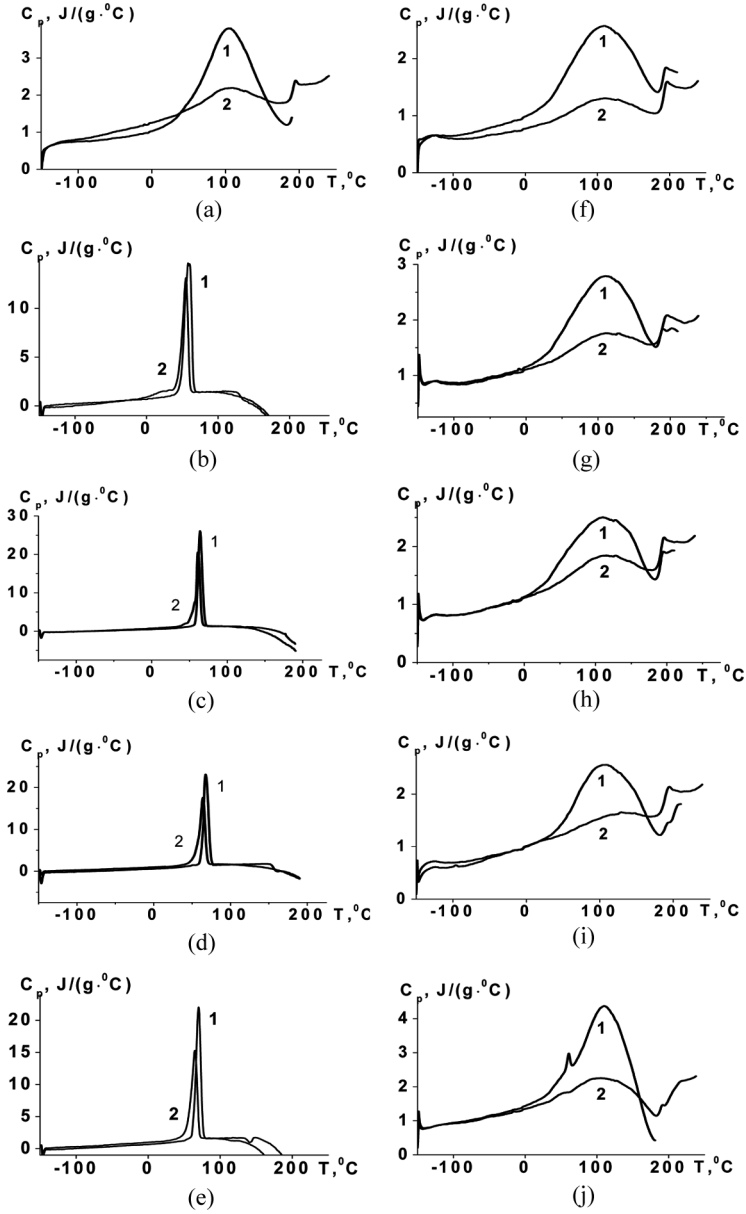

FIGURE 2 DSC thermograms for PAAm (a), PEG1 (b), PEG 2 (c), PEG 3 (d), PEG 4 (e), TBC1 (f), TBC2 (g), TBC3 (h), TBC4 (i), TBC5 (k), 1st scan – 1 and 2nd scan – 2.

TABLE 2 Parameters of Structural Transitions in Homopolymers and Triblock Copolymers

Polymer	Scan	T_g[a], °C	ΔT_g[b], °C	ΔC_p[c], J·(g·°C)$^{-1}$	T_g^*[d], °C	T_m[e], °C	ΔT_m, °C	ΔH_m[f], J·g^{-1}	X_c[g], %
PAAm	2	190.9	8.0	0.55	–	–	–	–	–
PEG1	1	–	–	–	–	58.0	78.0	157.6	80
	2	–	–	–	–	55.0	105.1	141.1	72
PEG2	1	–	–	–	–	64.0	78.0	171.0	87
	2	–	–	–	–	61.0	100.0	162.9	83
PEG3	1	–	–	–	–	68.0	78.0	172.1	87
	2	–	–	–	–	64.0	100.0	164.0	83
PEG4	1	–	–	–	–	70.0	101.0	172.3	88
	2	–	–	–	–	65.0	100.0	156.3	79
TBC1	2	190.8	9.0	0.55	184.8	–	–	–	–
TBC2	2	187.6	11.9	0.54	182.4	–	–	–	–
TBC3	1	188.5	11.3	0.48	181.3	–	–	–	–
		202.5	7.4	0.04					
	2	196.0	9.7	0.56		–	–	–	–
TBC4	1	187.2	9.3	0.24	181.1	–	–	–	–
		202.0	8.5	0.34					
	2	188.0	12.3	0.57		–	–	–	–
TBC5	1	–	–	–	182.3	60.9	24.0	60.7	31
	2	187.0	6.6	0.33	–	56.1	30.0	18.6	10
		204.6	20.8	0.72					

[a]The glass transition temperature.
[b]The temperature interval of a structural transition.
[c]The heat capacity jump.
[d]The glass transition temperature of compatible blends of PEG + PAA calculated by Couchman-Karasz equation.
[e]The melting temperature.
[f]The melting enthalpy.
[g]The crystallinity degree: for pure PEG $X_c = \Delta H_m / \Delta H_m^0$, where ΔH_m^0 is the melting enthalpy for 100% crystalline polymer (196.8 J·g^{-1}) [11]; for TBC $X_c = \Delta H_m / (\Delta H_m^0 \cdot w_{PEO})$ [12], where w_{PEO} is the mass fraction of PEO in TBC.

[15]. This indicates an important role of the mobility of long side branches in the central block crystallization. On the other hand, the phenomena of the T_m depression and the X_c reduction for a crystallizable component (up to the full loss of its crystalline properties) is well-known in the blends of chemically complementary polymers [16,17], which is caused by their interaction. In the case of TBCs, the structural studies of the corresponding polymer blends can be used as a criterion for the prevailing influence of the first or second factors. Actually, if the loss of the ability to crystallize by one of the TBC components is caused by a special arrangement of the crystallisable and

amorphous blocks, then the crystalline properties of the given component would be restored in a corresponding physical mixture [6,15]. When the second factor is dominated, the analogous (to TBC) changes in properties of the crystallisable component would be observed in the polymer blends. DSC data for the PEG + PAAm mixtures with compositions equal to those of TBC1 and TBC4 are resulted in the study [9]. They testify to the T_m depression (by 5–8°C) and an X_c decrease (by 8–20%) of PEG in the initial blends (the 1-st scan) and also to the almost full absence of crystalline areas in the blends passed through a melt (the 2-nd scan). Thus, an important conclusion about a determining contribution of the polymer block interaction to a change of PEO crystalline properties in the TBC structure has been achieved.

The state of TBC amorphous areas is characterized by the parameters of glass transitions in Table 2. Note that only a single glass transition temperature for the samples TBC1,2 with rather short PEO and PAAm blocks was found. However, two glass transitions were observed for TBC3 at first on the 1-st scan of DSC thermograms (Fig. 2h,i) and then on the 2-nd scan (Fig. 2j), which indicates the microphase separation in the amorphous areas of the copolymer structure [15]. Analogously to the discussion in [9], the first glass transitions, whose temperatures are lower than T_g of PAAm (Table 2) but higher than that of PEO ($T_g = -57$°C), can be attributed to the regions of the full compatibility of polymer components, where PEO and PAAm segments are hydrogen-bound. The second transition with a temperature higher than T_g of PAAm can be related to the domains formed by ≪superfluous≫ segments of PAAm in TBC which doesn't interact with PEO. The relative growth of ΔC_p for the second glass transition shows that an increase in the PEO (and PAAm) block length results in an increase of the relative number of these domains in amorphous regions of the TBC structure (Table 2). In order to confirm the reference of the first T_g in the TBC structure to the regions of compatibility of PEO and PAAm segments, the expected (theoretical) values of T_g^* for compatible blends with the same compositions as those in the specific TBC samples were calculated, by using the Couchman-Karasz relation [18]:

$$\ln\left(\frac{T_g^*}{T_{g1}}\right) = \frac{w_2 \cdot \Delta C_{p2} \cdot \ln(T_{g2}/T_{g1})}{w_1 \cdot \Delta C_{p1} + w_2 \cdot \Delta C_{p2}}.$$

Here, w_1 and w_2 are the mass fractions of PEO and PAAm in TBC, but T_{g1}, T_{g2}, and ΔC_{p1}, ΔC_{p2} are, respectively, the glass transition temperatures and the heat capacity jumps for PEO and PAAm. Note

that the parameters of the glass transition for PEG cannot be determined from our experiments. That is why the values of $T_{g1} = -57°C$ and $\Delta C_{p1} = 0.25\,J/(g \cdot °C)$ established for PEO with $M_v > 1000$ in the studies [19,20] were taken for calculations. The T_g^* numbers found in such a way (Table 2) were in good accordance with T_g values corresponding to the first glass transition in TBCs.

The WAXS profile for PAAm (Fig. 3a) containing two diffusive overlapped maxima was in full accordance with the data in [21] and was attributed to the presence of two systems of planes of a paracrystalline lattice in the amorphous PAAm structure [11].

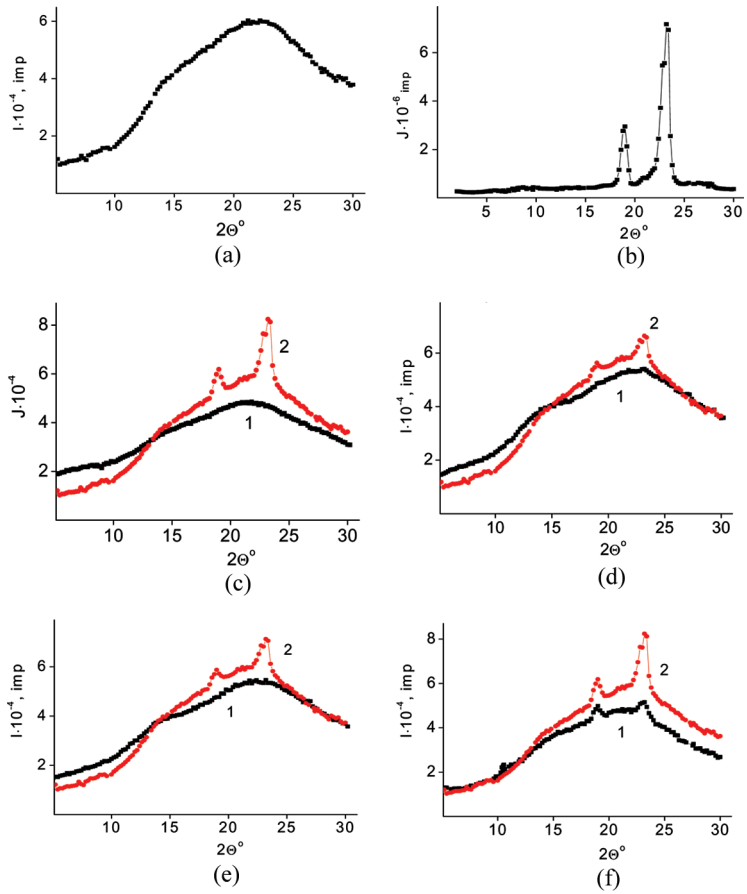

FIGURE 3 Difractograms for PAAm (a), PEG2 (b), TBC1 (c), TBC6 (d), TBC7 (e) and TBC5 (f). Experimental data – 1 and the additive curves calculated – 2. T = 25°C.

The first maximum with a smaller intensity ($2\theta \sim 15^\circ$) characterized the lateral periodicity in an arrangement of PAAm chains [11]. The second one with a greater intensity ($2\theta = 22.1^\circ$) was caused (according to the data of FTIR spectroscopy [9]) by a periodic arrangement of the flat hydrogen-bound *cis*-dimmers of amide groups in the structures of *cis-trans*-multimers. Similar two maxima (with smaller and greater intensity) were revealed in the diffractograms of some amorphous polymers having the flat side substitutes such as polystyrene and poly(vinyl carbazole) [11]. The average interplane distances in the paracrystalline lattice of PAAm found from the ratio $d = \lambda/(2\sin\theta)$ are represented in Table 3.

The WAXS profile of PEG (one example is shown in Fig. 3b) demonstrated two intense crystalline peaks at $2\theta = 19.0^\circ$ and 23.1° which are well known from the literature [11,16]. The profiles of the copolymers under study (Fig. 3c–g, curves 1), excepting TBC5, didn't contain the crystalline peaks in spite of the appearance of such peaks in the corresponding additive curves which were calculated for the PAA + PEG blends (curves 2) having the same compositions as those in specific TBC samples under the assumption about independent contributions of the components to the total scattering intensity. Small crystalline peaks of PEO were observed at the above-mentioned values of 2θ only in the TBC5 profile. However, their intensity turned out to be less than that in the additive curve. The full correlation of these results with DSC data is obvious. Using the Methues method, it is possible to calculate the ratio of the area of crystalline peaks to the area under the total WAXS curve and to find the so-called relative crystallinity degree for a homopolymer [11,13]. However, in the case of heteropolymers, the determination of this appropriate parameter loses any sense. Therefore, in order to estimate the changes in the crystallinity degree of PEO in the TBC5 structure, we calculated the ratio of the

TABLE 3 Positions of Maxima in WAXS Profiles and Corresponding Interplane Distances

	Positions of the diffraction maxima		The average interplane distances	
Polymer	$2\theta_1$, °	$2\theta_2$, °	d_1, nm	d_2, nm
PAAm	~15	22.10	~0.590	0.402
TBC1		21.60		0.411
TBC6		22.26	~0.590	0.399
TBC7	~15	22.56		0.394
TBC5		21.74		0.408

areas of the crystalline peaks in additive curve 2 and experimental curve 1 (Fig. 3g). According to such a procedure, the crystallinity degree of initial PEG decreased in the TBC5 structure by 2.9 times, which is in agreement with a reduction of the X_c value in TBC5 (as compared to PEG4) by 2.8 times established by the DSC method in the 1-st scan.

The WAXS profiles for amorphous TBCs were similar to diffractograms of pure PAAm. Some difference consisted in an appreciable reduction of the relative intensity of the second maximum and in the alteration of its position (Fig. 3, Table 3). This effect suggests changes in the disposition of *cis*-dimmers of amide groups in the structures of *cis-trans*-multimers of TBCs. The interaction of PEO and PAAm blocks in TBC should be reflected also in changes of the lateral periodicity in the macrochain arrangement, as it was observed in the structure of InterPC formed by PEG and poly(acrylic acid) [16]. However, such information cannot be obtained from the data of Figure 3 because of the uncertain position of the first maxima in the WAXS profiles of PAAm and TBCs.

Unlike WAXS, which is used to probe a block copolymer structure on the length scale of the crystalline or paracrystalline unit cell, the small-angle X-ray scattering (SAXS) allows investigating the morphology of block copolymer at the level of the microphase-separated structures [11,14]. SAXS profiles obtained are shown in Figure 4. A sharp decay of the scattering intensities

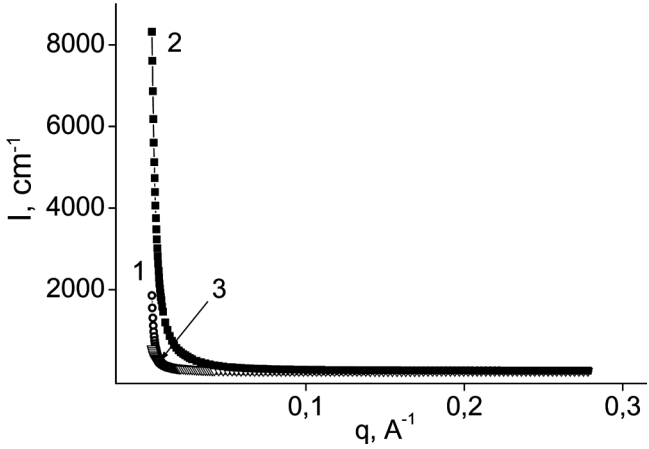

FIGURE 4 Intensity of small-angle X-ray scattering *vs* the wave vector for PAAm – 1, TBC6 – 2, and TBC5 – 3. T = 25°C.

versus the wave vector without appearance of any peaks or halos is observed for all the polymer samples. This fact suggests the absence of any periodicity in a disposition of separate structural elements of PAAm and TBCs (similar to the paracrystalline lattice) at a supramolecular level. The same profiles were represented then in two logarithmic coordinates (Fig. 5) for the detailed analysis according to the known conception about the formation of fractal aggregates or clusters [21,22]. A linear reduction of log$I(q)$ on log$q$ (the scattering regime by Porod [21]) with alone slope (Fig. 5a) was observed for PAAm (curve 1) and TBC samples with relatively short PEO chains (curves 2 and 3). The slope moduli reflecting the fractal dimension P_i ($P_i = 2.7$ for PAAm, and 2.3 and 2.4 for TBC1 and TBC3, respectively) were found to be less than 3. Such a behavior means the existence of mass-type fractal clusters [21,16] in the amorphous structure of PAAm and TBC samples. Unlike this, the double logarithmic SAXS profiles for TBC4 and TBC5 (Fig. 5b), which contained long enough PEO chains, demonstrated two linear parts with different slopes (two Porod's regimes) and some intermediate region between them (the scattering regime by Gineau [21]). The numbers of P_i turned out to be 2.8–3.1 in the 1-st Porod's regime (at higher q) and 2.4 in the 2-nd Porod's scattering regime (at less q) for both TBCs. Taking into account the above data of DSC and WAXS, these results can be interpreted by the appearance of nanocrystalline domains of PEO segments [21] among the mass-fractal clusters in TBC4 anf TBC5 structures. Using the inflection points of curves 4 and 5 in Figure 5b, the

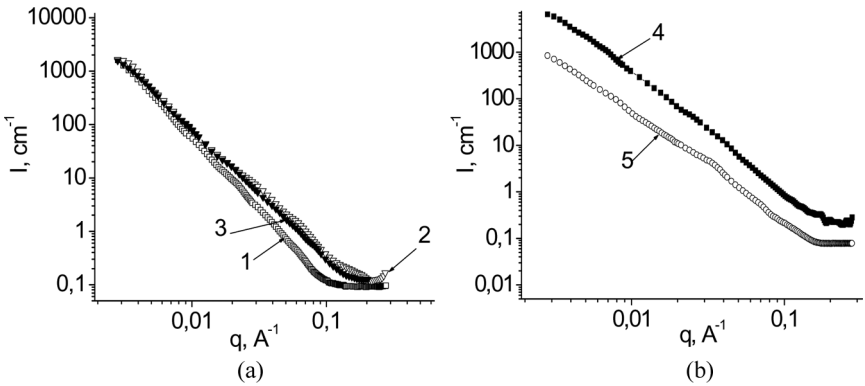

FIGURE 5 Intensity of small-angle X-ray scattering *vs* the wave vector in double logarithmic coordinates for PAAm – 1(a), TBC1 – 2(a), TBC6 – 3(a), TBC7 – 4(b), and TBC5 – 5(b).

average diameter of nanocrystalline domains was evaluated ($d_{av} \sim 2\pi/q$). It was equal to ~18 nm for both TBCs.

CONCLUSION

Thus, formation of IntraPC in macromolecules of TBC prevents the crystallization of PEO and provides the existence of a homogeneous amorphous copolymer structure composed of the one-level mass fractals in a wide range of the molecular weight changing of both the blocks. At the same time, at an excessively high length of the blocks (as in TBC7 and TBC5), the infringement of the TBC structural homogeneity took place due to a partial crystallization of PEO and the appearance of a microphase separation in amorphous regions. In this case, two levels of the TBC supramolecular structure organization including primary and branched mass fractal clusters were displaced.

REFERENCES

[1] Hamley, I. W. (1999). *The Physics of Block Copolymers*, Oxford Univ. Press: Oxford.
[2] Riess, G. (2003). *Prog. Polym. Sci.*, *28*, 1107–1170.
[3] Soo, P. L. & Eisenberg, A. (2004). *J. Polym. Sci., Part B: Polym. Phys.*, *42*, 923.
[4] Goloub, T., de Keizer, A., & Cohen Stuart, M. A. (1999). *Macromolecules*, *32*, 8441.
[5] Zheltonozhskaya, T., Demchenko, O., Rakovich, I., Guenet, J.-M., Syromyatnikov, V. (2003). *Macromol. Symp.*, *203*, 173.
[6] Xie, H.-Q. & Xie, D. (1999). *Prog. Polym. Sci.*, *24*, 275.
[7] Zheltonozhskaya, T. B., Zagdanskaya, N. E., Demchenko, O. V., Momot, L. N., Permyakova, N. M., & Syromyatnikov, V. G. (2004). *Russ. Chem. Rev.*, *73*, 811.
[8] Momot, L. N., Zheltonozhskaya, T. B., Permyakova, N. M., Fedorchuk, S. V., & Syromyatnikov, V. G. (2005). *Macromol. Symp.*, *222*, 209.
[9] Permyakova, N. M., Zheltonozhskaya, T. B., Shilov, V. V., Zagdanskaya, N. E., Momot, L. N., & Syromyatnikov, V. G. (2005). *Macromol. Symp.*, *222*, 135.
[10] Dolgoplosk, B. A. & Tynyakova, E. I. (1972). *Redox Systems as Sources of Free Radicals*, Nauka: Moscow, [in Russian].
[11] Lipatov, Yu. S., Shilov, V. V., Gomza, U. P., & Kruglyak, N. E. (1982). *X-Ray Diffraction Methods to Study Polymeric Systems*, Naukova Dumka: Kyiv, [in Russian].
[12] Vonk, C. G. (1975). *J. Appl. Crystallogr.*, *8*, 340.
[13] Pielichowski, K., Flejtuch, K., & Pielichowski, J. (2004). *Polymer*, *45*, 1235.
[14] Hamley, I. W. (1999). *Adv. Polym. Sci.*, *148*, 113.
[15] Privalko, V. P. & Novikov, V. V. (1995). *The Science of Heterogeneous Polymers. Structure and Thermophysical Properties*, Wiley: Chichester.
[16] Lipatov, Yu. S., Shilov, V. V., Gomza, U. P., Bimendina, L. A., & Bekturov, E. A. (1981). *Dop. AN URSR. Ser. Khim.*, *52*.
[17] Kuo, S. W. & Chang, F. C. (2001). *Macromolecules*, *34*, 4089.
[18] Nesterov, A. E. (1984). *Properties of Solutions and Polymeric Blends. 1*, Naukova Dumka: Kyiv, [in Russian].

[19] Privalko, V. P., Lipatov, Yu. S., Lobodina, A. P., & Shumskiy, V. F. (1974). *Vysokomol. Soedin. Ser.*, *16*, 2771.
[20] Privalko, V. P. & Lobodina, A. P. (1974). *Polym. J.*, *10*, 1033.
[21] Shpak, A. P., Shilov, V. V., Shilova, O. A., & Kunitsky, Yu. A. (2004). *Diagnostics of Nanosystems. Multilevel Fractal Structures*, Kyiv.
[22] Korolev, U. M., Veretyahina, T. G., Chupov, V. V., Valuev, L. I., & Plate, N. A. (1995). *Vysokomol. Soedin. Ser. A*, *37*, 1160.